ADVANCED ELECTRONIC MATERIALS Open Access
www.advelectronicmat.de

High-Throughput Production of Electrically Conductive Yarn (E-Yarn) for Smart Textiles

Jonas Marten, Nathalie Gaukel, Yunkai Hu, Yiliang Wang, Guangjie Yuan,* and Norbert Willenbacher*

Electrically conductive yarn is essential for developing smart textiles, combining advanced functionalities with the desirable mechanical properties of traditional yarn. This study introduces an innovative method for manufacturing Nylon yarn coated with an electrically conductive, thermoplastic polymer layer. The method is based on the classical wire coating process, thus enabling rapid scale-up. The feasibility of the new approach is demonstrated by coating a Nylon yarn 250 µm in diameter with a 20 µm thermoplastic coating layer consisting of a polyamide (Platamid M1276 F, melting temperature 110–120 °C) matrix including 20 vol% silver flakes (d_{50} 2.5 µm). The resultant resistivity of the coated yarn is ≈7.5 Ω cm^{-1}, and essentially kept constant even after multiple bending and washing cycles simulating typical stresses during textile utilization. Additionally, the yarn is used to fabricate a pressure sensor, demonstrating a pressure sensitivity range of 1–20 kPa, a sensitivity of 10^{-3} kPa^{-1}, and a response time of 224 ms. This study showcases a versatile manufacturing process for electrically conductive yarn suitable for smart textile applications. It emphasizes the potential for integrating these yarns into functional textile systems and highlights the feasibility of using existing industrial-scale coating equipment, thus facilitating rapid market integration.

1. Introduction

Smart textiles represent an emerging frontier with immense potential across various domains of next-generation wearable electronics. These versatile materials find utility as pressure sensors for human motion,[1] artificial muscles for soft robotics,[2] electromagnetic interference shields,[3] and serve broader functions as electrical sensors, actuators, supercapacitors, energy harvesters, or displays,[4–6] Deployment methods include screen-printing or direct ink writing of conductive pastes, and the use of 3D printable electrically conductive filaments directly onto the fabric.[5,7,8] However, a smoother integration of conductivity into the traditional fabric manufacturing process can be realized by directly applying the electrically conductive material to the fiber or yarn. Additionally, this approach ensures that the fabric retains its original mechanical properties, such as elasticity and flexibility.[9] The most common way of manufacturing electrically conductive fabric involves weaving, knitting, or sewing metal wires in addition to conventional yarn,[10,11] while alternative approaches entail applying metal films via techniques like sputtering, electrodeless plating, or screen-printing directly on the yarn.[12–14] Moreover, methods such as dip-coating, spray-coating, or drop-coating enable the application of thin layers of conductive materials like silver (Ag) nano-wires or single-walled carbon nanotubes (CNT) to yarn surfaces, offering an relatively easy to handle process with the ability to adapt to specific product requirements by varying the conductive materials.[15–17]

Although these methods supply electrically conductive yarn with suitable properties for manufacturing e-textiles, one key factor is overlooked frequently: a high-throughput manufacturing process that can effectively meet the demands of the textile industry. A process that enables the use of different kinds of raw materials regarding costs and properties, that is easy to handle,

J. Marten, N. Gaukel, N. Willenbacher
Institute for Mechanical Process Engineering, and Mechanics
Karlsruhe Institute of Technology
76131 Karlsruhe, Germany
E-mail: jonas.marten@kit.edu

The ORCID identification number(s) for the author(s) of this article can be found under https://doi.org/10.1002/aelm.202400700

DOI: 10.1002/aelm.202400700

Y. Hu, G. Yuan
School of Mechatronic Engineering and Automation
Shanghai Key Laboratory of Intelligent Manufacturing and Robotics
Shanghai University
Shanghai 200444, China
E-mail: guangjie@shu.edu.cn

Y. Wang
Research and Development Department
Jinjing (Group) Co., Ltd
Shandong 255022, China

energy efficient, and provides flexibility to adapt quickly to a dynamic textile market. To fill this gap, we have developed a versatile alternative to the conventional coating techniques mentioned above, using a polymer solution-based coating process similar to the insulation coating of thin copper wires for use in electromagnetic coils.[18] The similarity to this already well-established coating technique enables a quick scale-up with the possibility of a high-throughput, energy-efficient yarn production at an output of up to 800 m min^{-1} based on well-established coating equipment. The inks utilized here are formulated akin to those employed in wire coating processes, comprising a polymeric compound dissolved in a compatible solvent, filled with electrically conductive particles. The selected components (solvent, polymer, filler) provide the basis for a modular system that enables different functional layers to be applied to a variety of different yarns or filaments in a stable, efficient, and fast-working process and offers the possibility of making rapid changes to the formulation without the need to develop new application methods. To demonstrate the strategy, a polyamide-based coating filled with silver particles was used to apply thin electrically conductive coating layers to a Nylon yarn using a customized laboratory-scale coating machine. Washing and bending tests were employed to demonstrate the durability of the yarn with its electrically conductive coating when exposed to stresses typically occurring during utilization. Subsequently, the conductive yarn was used to manufacture a deformable capacitive pressure sensor. The obtained sensor signal was evaluated with respect to its sensitivity, linearity, characteristic response time, and cyclic stability. Finally, the feasibility of the electrically conductive coated yarn for smart textile applications is discussed.

2. Results and Discussion

2.1. Coating Process

To manufacture coated yarn, a laboratory scale coating machine was customized. **Figure 1** illustrates the process of applying a single coating layer to the yarn using this machine at a maximum speed of 6.9 m min^{-1}. The machine consists of several key components, as displayed in Figure 1a: 1) a freely rotating spool loaded with the bare yarn, 2) a coating nozzle for the precise application of the silver-filled polymer solution, 3) an oven used to dry the wet-coated yarn, 4) a cooling station where the silver-filled polymeric coating is cooled down and 5) a spool directly connected to a motor winds the coated yarn. Figure 1b shows a magnification of the wet-coating application segment. It consists of a guiding nozzle marginally larger than the yarn, guiding its path. A reservoir, filled with the silver-filled polymer solution using a syringe and a coating nozzle that controls the thickness of the wet coating applied to the yarn. Figure 1c shows a commercially available coating nozzle commonly employed in conventional wire coating processes. These nozzles feature variable core drilling diameters, typically ranging from 100 to 800 µm for this specific type. Figure 1d schematically shows the wet-coating application of a polymer solution filled with silver particles onto the yarn within the coating nozzle, followed by a drying step to remove the solvents, as sketched in Figure 1e. The result is a thin solid polymer layer filled with an electrically conductive silver particle network. The coating thickness after a single application ranges between 2 and 7 µm, depending on the dry content of the polymer solution. By repeating these coating steps using guiding and coating nozzles with appropriately increasing diameter, several coating layers can be applied on top of each other, enabling the precise adjustment of the coating thickness. Even composition gradients can be tailored using different polymer solutions, e.g., with different fillers, in subsequent coating steps. In the wire coating industry, several nozzles with slightly increasing diameters are connected enabling a quick layer buildup.[18] An industrial coating machine is described in more detail in Figure S1 (Supplementary Information).

To formulate composite polymer solutions that yield good coating properties and high electrical conductivity, we first investigated the electrical properties of the dry coating layer after solvent evaporation (**Figure 2**). Next, the solvent content and consequently the viscosity of the silver-filled polymer solutions were adjusted (**Figure 3**), and finally, coating trials were performed.

2.2. Electrical Characterization of the Coating Material

The dry coating layer (Figure 1e) is a composite material including a mixture of polyamide and the ionic liquid (IL) 1-Butyl-3-Methyl-imidazolium iodide, filled with silver particles. At the low filling level desired here, a uniform distribution of the silver particles in the polymer matrix would result in low conductivity. Thus, the IL is added to promote the formation of a percolating particle network during the drying process. The IL partially removes the isolating fatty acids from the silver flakes and causes a microphase separation, which induces the formation of an electrically conductive network and hence increases the electrical conductivity of the resulting coating.[5,8,19,20] Accordingly, the electrical conductivity of the composite depends on the volume fraction of the added silver as well as on the volume ratio of IL to Ag. Corresponding conductivity data are shown in Figure 2. The electrical conductivity of coatings with a constant Ag fraction of 20 vol% but increasing IL concentration is shown in Figure 2a). Conductivity drastically increases at V_{IL}/V_{Ag} ratios between 0.02 and 0.04 reaching κ values ≈1000 S cm^{-1}, and a further slight increase in conductivity is observed at higher IL content. An excessive IL concentration, however, can result in the formation of large Ag agglomerations, as evidenced in Figure S2 (Supplementary Information). This can lead to nozzle blockage during the coating process and results in an uneven coating. Thus, for subsequent investigations, the formulation with a V_{IL}/V_{Ag} ratio of 0.04 was chosen. This ratio yielded a commendable conductivity of ≈812 S cm^{-1} at 20 vol% Ag content while avoiding the formation of large agglomerates. Figure 2b shows the conductivity of the dry coating layers as a function of silver content, maintaining a constant ratio of V_{IL}/V_{Ag} = 0.04. At silver fractions of 12, 16, and 20 vol%, the measured conductivities were ≈498, 689, and 812 S cm^{-1}, respectively. These findings highlight the IL's effectiveness in promoting the formation of a percolating silver particle network, even at low Ag fractions within the dry coating. Typically, the percolation threshold, i.e., the filler concentration at which formation of a continuous, sample-spanning particle network and hence a significant conductivity set in, for similar silver particle-filled polymer films, falls between 20 and 30 vol%.[21] Additionally, when compared

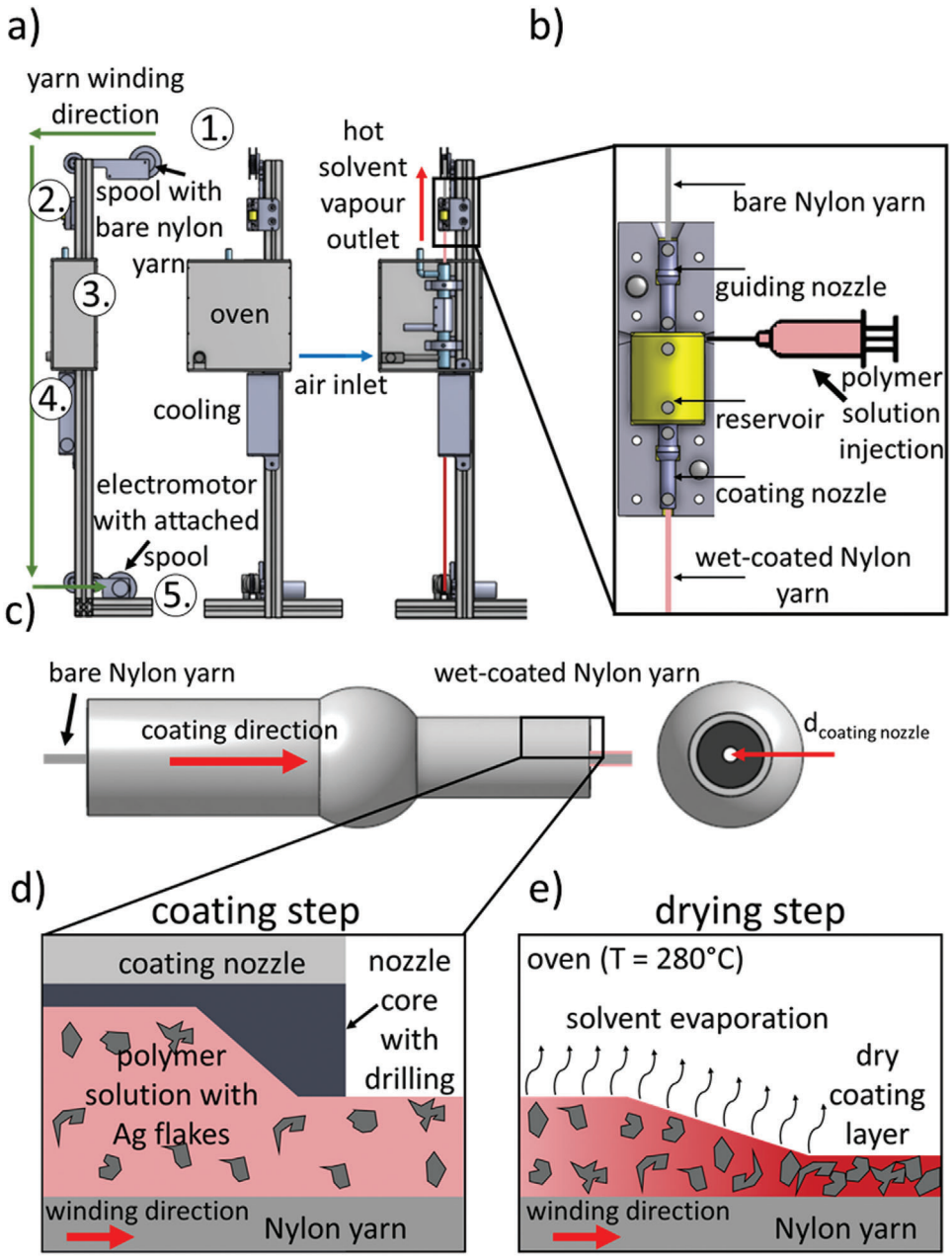

Figure 1. Description of the yarn coating process. a) A self-constructed, continuously operating laboratory-scale coating device capable of achieving a maximum coating speed of 6.9 m min^{-1}. The device includes the following key components: 1) a freely rotating spool for the bare yarn, 2) a coating nozzle, 3) a drying oven, 4) a cooling station, and 5) a winder and spool for the coated yarn. The green arrows indicate the coating direction. b) A magnification of the wet-coating application segment. c) A coating nozzle commonly employed in conventional wire coating processes. d) Wet-coating application with a polymer solution filled with silver particles onto the yarn. e) A subsequent drying step to remove the solvents.

to results for Ag nano-wire (NW) coated yarn with maximum conductivities of ≈81[22] and 300 S cm^{-1},[17] and a ratio V_{IL}/V_{Ag} = 0.04. The formulation containing 20 vol% Ag was selected to achieve a high electrical conductivity of the resulting yarn and still provide sufficient mechanical durability in typical applications. A higher particle content in the coating would result in a higher conductivity but would at the same time reduce adhesion and compromise long-term stability. Formulations with lower Ag content are expected to have at least similar if not superior, mechanical reliability but, of course, yield a lower electrical conductivity.

2.3. Viscosity Adjustment of the Polymer Solution

After adjusting the dry content ratio (Ag, IL) in the polymer solution, it is also necessary to optimize the solvent concentration and, consequently, the viscosity of the polymer solution to

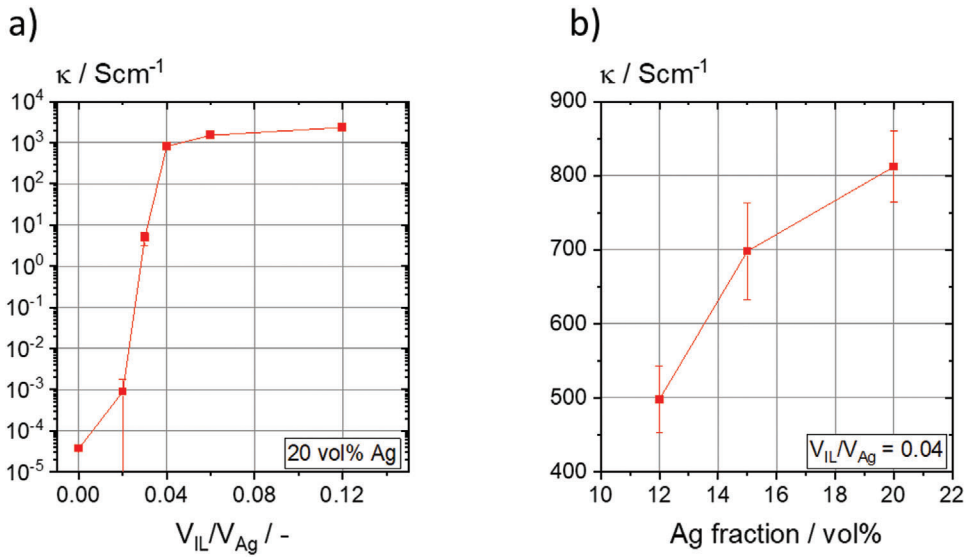

Figure 2. a) Electrical conductivity κ of solvent-free coatings with a constant Ag fraction of 20 vol%, plotted against the IL-Ag volume ratio. b) Electrical conductivity κ of solvent-free coatings with a constant IL-Ag volume ratio of 0.04, plotted against the Ag volume fraction.

achieve high surface quality. Initially, the impact of adding Ag and IL on the viscosity of a base polymer solution with a polymer concentration of 15 wt% was investigated, as depicted in Figure 3a. The polymer solution exhibits purely Newtonian behavior, with a viscosity of ≈0.1 Pa·s within the observed shear rate range of 1–100 s^{-1}. Introducing particles results in a slight viscosity increase. Additionally, the silver-filled formulation exhibits weak shear-thinning behavior within the observed shear rate range. Notably, the flow curve of the formulation containing IL alongside the particles exhibits similar behavior to that containing only particles. Furthermore, the formulation containing the same amount of IL but without particles shows only a slight increase in viscosity, from 0.1 Pa·s for the polymer solution alone to 0.108 Pa·s with the addition of IL. This increase is due to the IL's inherently higher viscosity of ≈0.39 Pa·s. The flow curve for IL is provided in Figure S3 (Supplementary Information). This

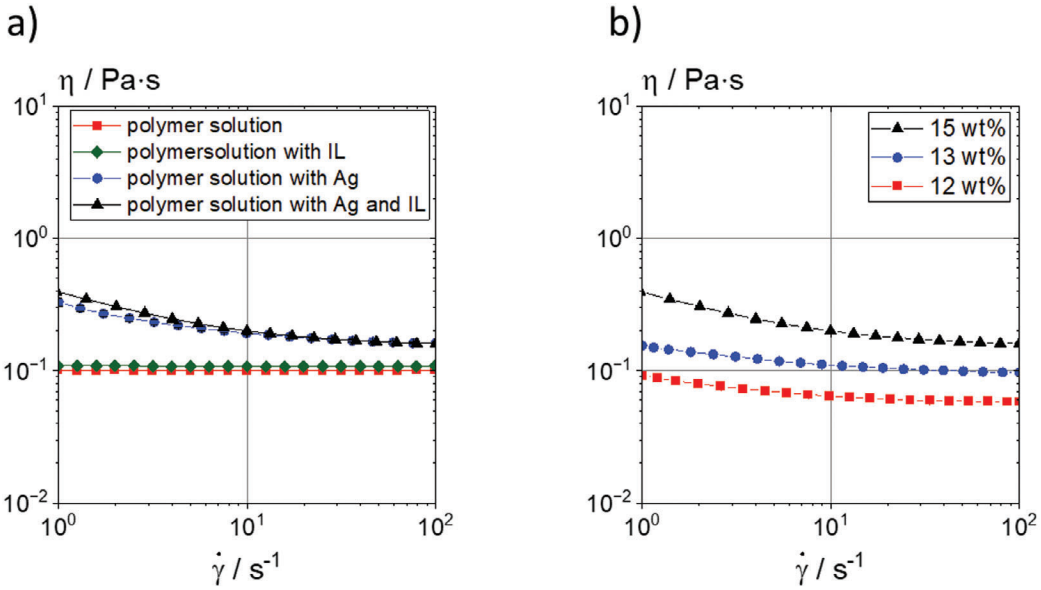

Figure 3. a) Viscosity η as a function of shear rate $\dot{\gamma}$ for various polymer solutions: the pure polymer solution at a concentration of 15 wt% (red squares), the polymer solution with silver particles comprising 20 vol% of the nonvolatile components (blue circles), the polymer solution with the same silver concentration as well as added IL with a V_{IL}/V_{Ag} ratio of 0.04 (black triangles), and the polymer solution containing the same volume of IL but no silver particles (green diamonds). b) Viscosity η as a function of shear rate $\dot{\gamma}$ for formulations including 20 vol% Ag (with respect to the nonvolatile components), maintaining a V_{IL}/V_{Ag} ratio of 0.04 but with different polymer concentrations in the base solution: 12 wt% (red squares), 13 wt% (blue circles), and 15 wt% (black triangles).

suggests that while the addition of IL induces microphase separation and particle network formation during the drying process in this system (see Figure S2, Supporting Information), it just slightly affects the viscosity of the initial polymer solution when using a V_{IL}/V_{Ag} ratio of 0.04.

Figure 3b displays the flow curves of formulations with an Ag fraction of 20 vol% with respect to the nonvolatile components and a V_{IL}/V_{Ag} ratio of 0.04 but different polymer concentrations of the base solution. As expected, the viscosity increases with increasing polymer concentration and at a shear rate of 10 s^{-1}, viscosity values of 0.2, 0.1, and 0.06 Pa·s, respectively, are found for base solutions with 15, 13, and 12 wt% polymer content. To facilitate the utilization of these formulations in traditional wire coating machines and thus achieve high-throughput production of conductive yarn, the viscosity of the polymer solutions should be >0.03 Pa·s, a criterion met in all three instances.[23]

2.4. Yarn Coating Trials

Yarn coating trials were conducted using solutions with 12, 13, and 15 wt% polymer concentrations. The coating process employed the coating machine illustrated in Figure 1. The coating speed was set to 2.8 m min^{-1}, while the oven temperature was maintained at 280 °C. It is important to note that the oven temperature could not be increased further without risking damage to the nylon yarn. **Figure** 4a–c displays the quality of yarn coatings for formulations containing 15, 13, and 12 wt% polymers in the base solution after four, four, and five coating cycles, respectively. Noticeable differences in surface quality are observed. Figure 4a shows numerous craters and bubbles along the Nylon yarn, resulting in a generally poor surface quality. However, as the polymer concentration decreases (as seen in Figure 4b), the surface quality improves, although occasional bubbles and craters persist. Given the unsatisfactory coating qualities observed with both 15 and 13 wt% polymer solutions, the process was halted after four coating cycles. Further reduction in polymer concentration to 12 wt% resulted in sufficient surface quality without defects, even after the fifth coating cycle (Figure 4c). It is likely that bubbles and craters form during the coating process because a solid polymer layer develops on the surface before all the solvent has evaporated. The trapped solvent beneath this layer continues to evaporate, building pressure until it deforms the polymer surface, resulting in bubble formation. As more solvent escapes, these bubbles can burst, leaving behind craters. This phenomenon is also observed in conventional wire coating processes.[18] The corresponding coating thicknesses in relation to the number of coatings are depicted in Figure 4d. The maximum measured coating thicknesses were ≈22 and 16 µm for Nylon yarn coated with polymer solutions containing 15 and 13 wt%, respectively. In contrast, the coating thickness of Nylon yarn coated with a formulation containing 12 wt% was ≈17 µm after five coating cycles. After each coating cycle, the electrical resistance of the yarn was measured, as illustrated in Figure 4e. As can be expected, for all three formulation types, resistance decreased with an increasing number of coatings, and hence thicker layers of conductive material on the yarn. The minimum resistance recorded for formulations containing 15 and 12 wt% polymer after four coating cycles was ≈21 and 17 Ω cm^{-1}, respectively. Notably, the formulation with 12 wt% polymers exhibited a resistance of ≈7.5 Ω cm^{-1} after five coating cycles, similar to results reported in other publications, with values between 0.2 and 20 Ω cm^{-1} for nano-wire coated yarns.[15,24] Further reduction in resistance could likely be achieved by either increasing the number of coatings or by increasing the silver concentration. Consequently, the process offers adaptability to adjust yarn resistance to the level required for different applications. Additionally, Figure 4f presents the cross-section of the Nylon yarn after five coating cycles with the formulation containing 12 wt% polymers and Figure 4g,h scanning electron microscopy (SEM) images of the coated yarn surface and the cross-section. The results show that it is possible to apply thin layers of an electrically conductive polymer film with sufficient surface quality at a relatively high speed of 2.8 m min^{-1} which could potentially be increased up to 800 m min^{-1} by using an industrial coating machine, as depicted in Figure S1 (Supplementary Information). This scale has previously been demonstrated for electrically conductive polymer films coated onto copper wires.[20] Moreover, an additional critical aspect is the solids content of the initial coating ink. In processes where silver and silver-coated copper nano-wires suspended in solvents were applied to yarn through dip-coating, substantial amounts of solvent were required, due to the limited dispersibility of nano-wires in solvents. In these cases, particle concentrations ranging from 1.25 to 8 mg mL^{-1} were used.[15,17,24] In contrast, the formulations employed in this study feature orders of magnitude higher solids concentrations, totaling 345 mg mL^{-1}, with 250 mg mL^{-1} attributed to silver and 95 mg mL^{-1} to the polymer component. Thus, the solvent consumption and hence the required drying energy is much lower, which makes this approach much more feasible for industrial application. The cost associated with the material itself is primarily determined by the cost of the Ag particles, resulting in an approximate price of 0.04 \$ m_{yarn}^{-1}, slightly higher than that reported for Ag nano-wire coated yarn ranging between 0.008 and 0.035 \$ m_{yarn}^{-1}.[24] While the cost for polymers filled with pure silver particles is slightly higher than for the metal nano-wire systems mentioned above, this approach offers the advantage of substituting silver particles with less expensive alternatives such as silver-coated copper or glass particles as suggested previously.[20] Additionally, Carbon Black (CB) or Carbon Nanotubes (CNT) could serve as alternative options, further reducing material expenses. As the polymer matrix provides both mechanical strength and adhesion to the yarn, the system does not rely on good adhesion between the conductive material and the yarn surface, as pointed out in previous studies focusing on metal nano-wire systems.[15,24] This characteristic opens up new possibilities, such as employing microparticles instead of nano-sized materials, thereby simplifying the production process since micron-sized particles are easier to handle and incorporate into formulations. Furthermore, applying coating layers containing different kinds of particles on top of each other could also be an option to attain specialized properties, such as conductivity gradients. Another option is to incorporate small amounts of micro or nano-sized pigments to color the yarn. This allows for tailoring the yarn's appearance according to customer preferences with minimal changes to the standard formulation.

Given that the best coating quality was attained utilizing a base solution comprising 12 wt% polymers, this specific yarn serves as the focus for subsequent investigations.

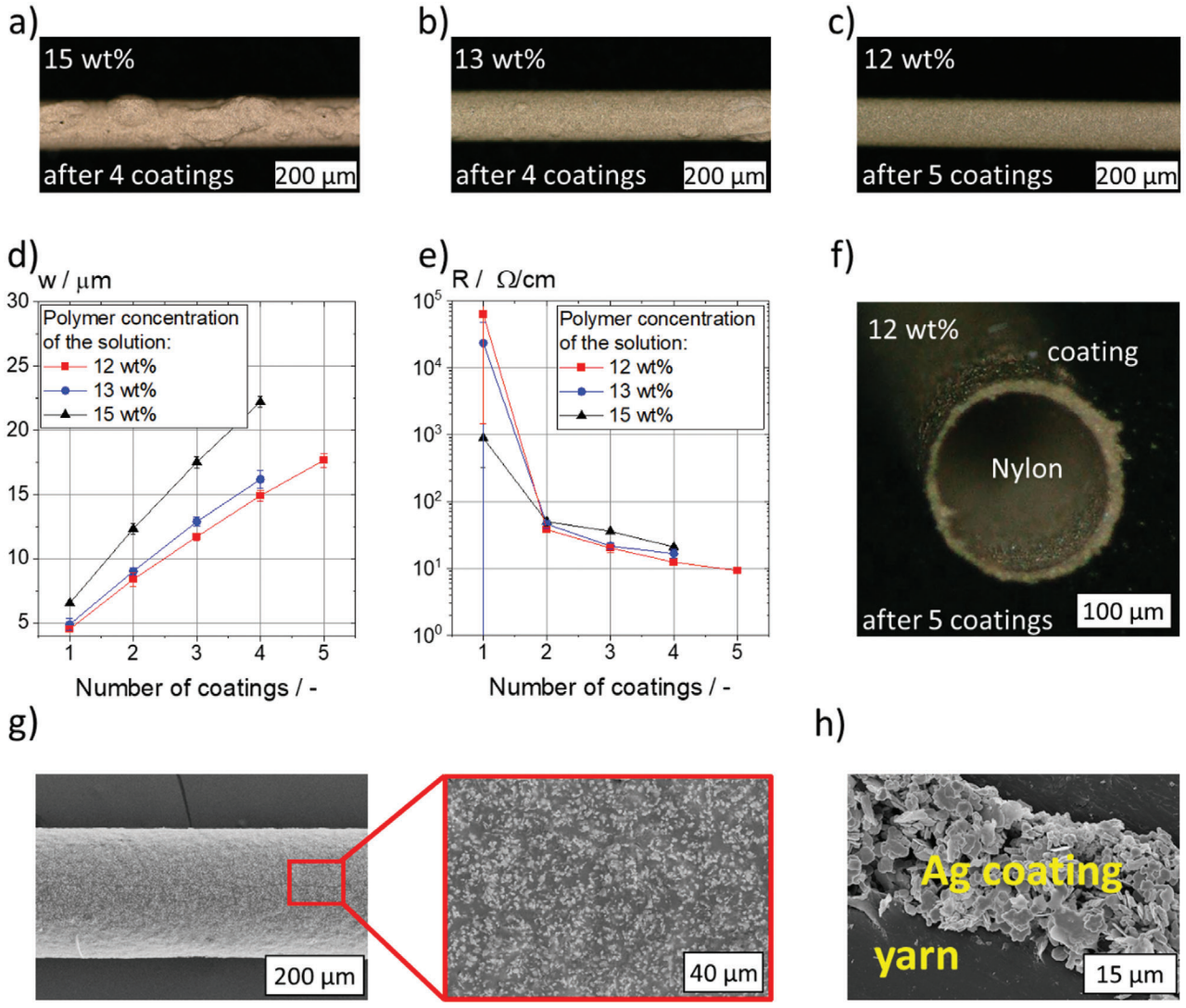

Figure 4. Light microscopy images of the surface of Nylon yarn coated with formulations containing 20 vol% Ag in the final dry film, a V_{IL}/V_{Ag} ratio of 0.04, and polymer concentrations of a) 15 wt%, b) 13 wt%, and c) 12 wt% in the base solution. Images were taken after four or five coating cycles, as depicted in the images. d) The coating thickness and e) the electrical resistance for Nylon yarn coated with Ag- and IL-filled formulations with 15 wt% (black triangles), 13 wt% (blue circles), and 12 wt% (red squares) polymer in the base solution, plotted against the number of coatings. f) light microscopy image of the cross-section, g) SEM image of the surface, including a magnification (surrounded by a red rectangle), and h) SEM image of the cross-section of Nylon yarn coated with the formulation containing 20 vol% Ag in the final dry film, a ratio $V_{IL}/V_{Ag} = 0.04$, and a polymer concentration of 12 wt% in the base solution. The images were taken after five coating cycles.

2.5. Washing and Bending Tests

Materials suitable for manufacturing flexible sensors and e-textiles must be able to withstand repeated washing and also bending. Accordingly, initial stability tests regarding these properties were conducted. **Figure** 5a shows the material resistance as a function of the number of washing cycles. Although the resistance slightly increases after the first washing cycling, from 7.5 $\Omega\ cm^{-1} \pm .5\ \Omega\ cm^{-1}$ to $\approx 10\ \Omega\ cm^{-1} \pm .6\ \Omega\ cm^{-1}$, it remains constant for the next four washing cycles, indicating a good washing resistance for this prototype material. Figure 5b presents the results of the bending tests. The resistance slightly increases from 7.5 $\Omega\ cm^{-1} \pm .5\ \Omega\ cm^{-1}$ to 8.3 $\Omega\ cm^{-1} \pm .7\ \Omega\ cm^{-1}$ after more than 3000 bends, this is still within experimental uncertainty thus demonstrating the very good mechanical durability of our conductive yarn. To further improve its performance, the yarn could be coated more than five times to improve the toughness of the conductive network or an additional protective layer could be added.

2.6. Application for Flexible Pressure Sensor

The simplest possible design was used to illustrate the applicability of the conductive yarn for flexible pressure sensors. The capacitive sensor consists of two pieces of conductive yarn (coating

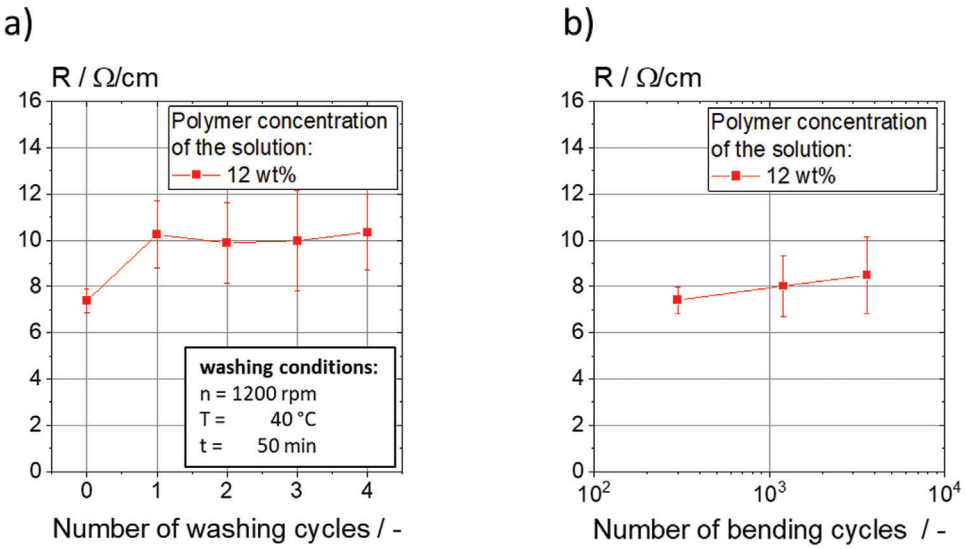

Figure 5. The electrical resistance of Nylon yarn coated with five layers of a formulation containing 20 vol% Ag in the final dry film, a ratio V_{IL}/V_{Ag} = 0.04, and a polymer concentration of 12 wt% in the base solution, plotted against the number of a) washing and b) bending cycles.

thickness = 20 µm, φ_{Ag} = 20 vol%, κ = 812 S cm^{-1}) separated by a layer of Ecoflex. Additional layers of polydimethylsiloxane (PDMS) are applied on the top and bottom to provide further protection, as shown in **Figure 6**a. By applying pressure to the surface of the sensor, the distance between the opposing yarn filaments decreases which leads to an increase in capacitance, as shown in Figure 6b.

Figure 7a–e illustrates the pressure-sensing functionality of the simple device. The conducted tests characterize the sensor specifications in terms of the changes in capacitance $\Delta C/C_0$ in response to a) increasing loading pressure, b) stepwise increasing increments in loading pressure, c) cyclic changes in loading pressure, d) duration of pressure application over time, and e) extended periods of pressure cycling. The results demonstrate that the sensor is capable of capturing the pressure range of 1–20 kPa (Figure 7a) which is adequate for capturing everyday activities such as handshakes, holding a mug, or conducting medical diagnoses.[25] With a sensitivity in the linear regime of 10^{-3} kPa^{-1} (Figure 7a) and a response time of 224 ms (Figure 7d), this sensor is in a similar specification range as other products, however, it is not among the best-performing ones with sensitivities of up to 217.5 kPa^{-1} and response times of sometimes <10 ms.[25–27] These preliminary tests show that the conductive yarn can be used for manufacturing sensors for integration into textiles, but further improvement is required for widespread technical application.

When more than two pieces of yarn are used, an array can be formed, as shown in **Figure 8**. This 5 × 5 yarn arrangement allows for the detection of the spatial distribution of small input pressure signals, enabling the sensor to distinguish not only the weight but also the shape of objects placed on it. This capability is demonstrated using two wooden blocks: a small one weighing 0.65 g (Figure 8a) and a larger one weighing 3.92 g (Figure 8b). The shape of the contact area between the block and the sensor layer can be retrieved from the spatial variation of the $\Delta C/C_0$ signal in the 5 × 5 matrix as shown in Figure 8 on the right. Of

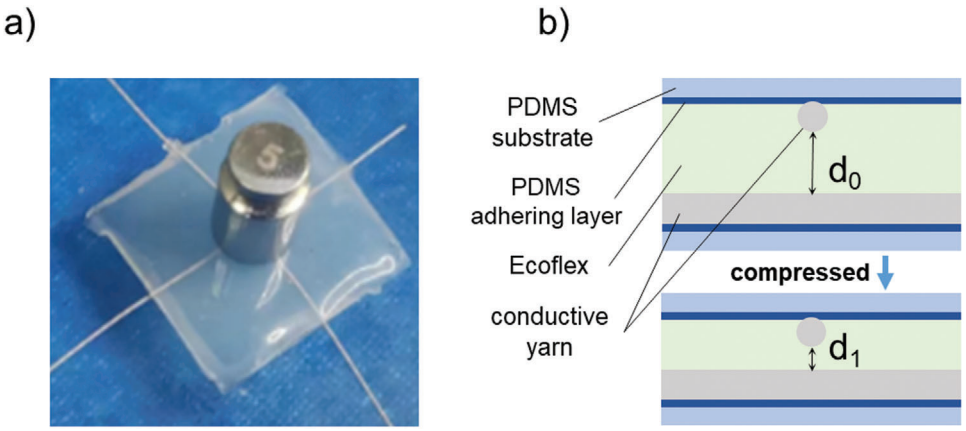

Figure 6. a) The flexible pressure sensor b) Working principle of the flexible pressure sensor.

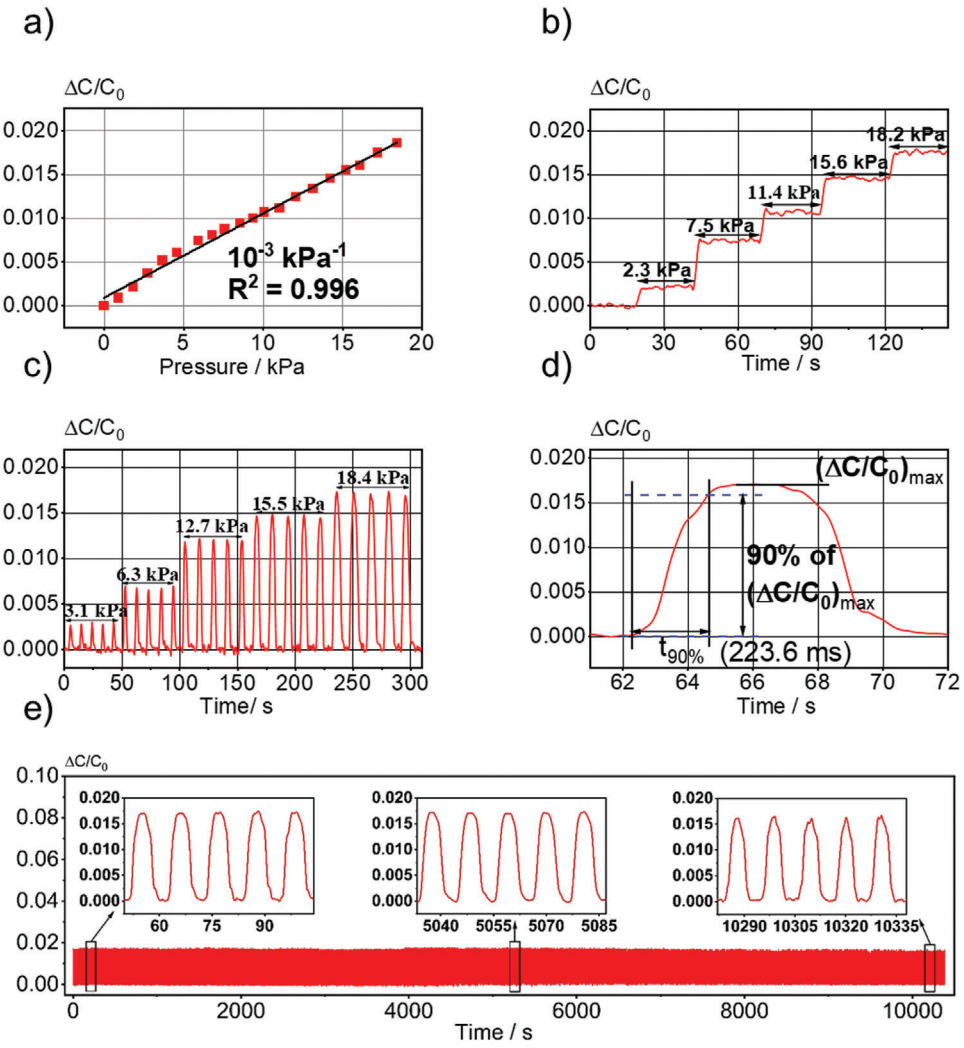

Figure 7. Sensing capability of the flexible pressure sensor: The relationship between $\Delta C/C_0$ and a) increasing loading pressure, b) stepwise increasing increments in loading pressure, c) cycling changes in loading pressure with peak loads of 3100, 6300, 12700, 15500, and 18400 Pa, d) duration of pressure application overtime at a pressure of 18 400 Pa, and e) extended periods of pressure cycling with 1000 loading-unloading cycles at a peak pressure of 18 400 Pa.

course, due to the simple layout, the spatial resolution is limited here, but further enhancement of the spatial resolution is straightforward by using more yarn at a smaller distance and also by using thinner yarn pieces.

Figure 9 illustrates the changes in capacitance when sensing a finger or just the fingertip under no pressure loading. Compared with the fingertip, the finger has a larger contact area on the surface of the sensor, which results in more capacitance drop. Therefore, the sensor can detect changes effectively as long as the finger or fingertip is near the electrode, which could be used in touch panels.

The change in capacitance during touch detection arises from the alteration in the edge electric field rather than from a change in the dielectric's size (Figure 9a). In this context, C_{total}, C_p, C_f, and C_d represent the total sensor capacitance, electrode plate capacitance, edge capacitance of the Ecoflex dielectric layer, and edge capacitance of the medium directly above the sensor, respectively. When no pressure is applied, the sensor remains physically undeformed, meaning C_p and C_f stay constant while C_{total} varies as C_d varies when the fingertip approaches the sensor surface. As depicted in Figure 9b when an object, e.g., the fingertip approaches the sensor, the edge electric field (the medium directly above the sensor) is redirected to the ground through the finger, causing a decrease in capacitance. Compared with the fingertip, the finger has a larger contact area on the surface of the sensor, which results in more capacitance drops. Therefore, the sensor can detect changes effectively as long as the finger or fingertip is near the electrode, which could be used in the application of touch panels.

3. Conclusion

This study presents an alternative production route for electrically conductive Nylon yarn immediately suited for upscaling to commercial-scale production capacities adequate for the textile industry, since it is based on a process similar to the industrial

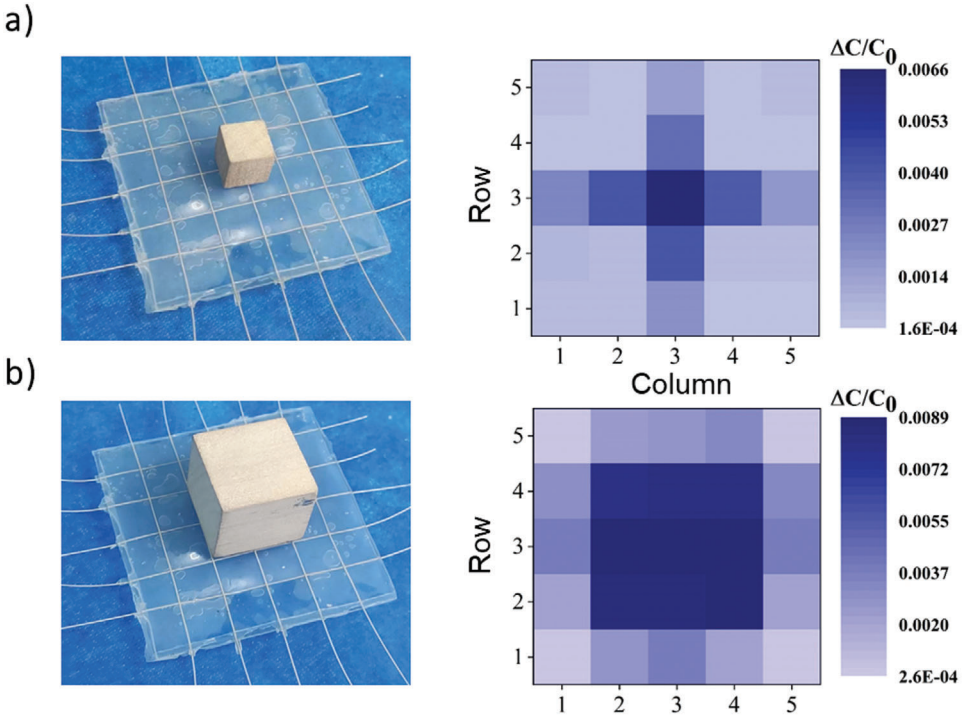

Figure 8. Spatial distribution of input pressure signals on a 5 × 5 yarn sensor array. Images and 2D intensity (ΔC/C0) map of the sensor with a) a small (0.62 g) and b) a large wooden block (3.92 g) placed at the center of the sensor array.

fabrication of insulated copper wires used in large quantities in the electrical industry.[18]

To demonstrate feasibility, a laboratory-scale coating machine was constructed to apply coating layers at a speed of 2.8 m min^{-1}. The coating ink used here is based on a solution of the thermoplastic polyamide Platamid M1276 F (T_M = 110–120 °C) in ethanol. Silver flakes (D_{50} = 2.5 µm) are suspended in this solution to provide electrical conductivity. Furthermore, 1-Butyl-3-Methyl-imidazoliumiodide, an ionic liquid, is added to further enhance conductivity.[8,20] After solvent removal, the final dry coating layer included 20 vol% silver, a V_{IL}/V_{Ag} ratio of 0.04, and provided a conductivity of 812 S cm^{-1}. Reducing the silver content to 16 vol% or 12 vol% resulted in conductivity values of 689 and 498 S cm^{-1}, respectively.

The viscosity of the coating ink is in the range of 50 mPa·s, and careful adjustment of the viscosity depending on coating speed and drying conditions is necessary to ensure high surface quality.[20] Here, a polymer concentration of 12 wt% in the base solution yielded the best results, producing a coating thickness of 17 µm after five coating cycles, with a resistance of 7.5 Ω cm^{-1}. Washing and bending tests were performed to assess the yarn stability in textile applications. Following several washing cycles and more than 3000 bending cycles, resistance marginally increased to 10 and 8.3 Ω cm^{-1}, respectively, indicating sufficient stability for textile applications considering the prototype level of development.

Initial tests were conducted using the conductive yarn in flexible, capacitive pressure-sensing applications. Based on the simplest design of two perpendicularly crossing filaments, we could show that the capacitance change $\Delta C/C_0$ is sufficient to detect pressures ranging from 1 to 20 kPa sufficient for typical everyday pressure scenarios. The sensitivity of the sensor is $\approx 10^{-3}$ kPa^{-1} with a response time of roughly 223.6 ms. Even after 1000 loading-unloading cycles at a pressure of 18.4 kPa, the sensor remained sensitive enough to accurately measure pressure differences. Additionally, a simple sensor layout with a rectangular 5 ×5-filament array could be used to demonstrate that spatial differences in capacitance change can be detected and may be used to detect pressure variations or the shape of objects in contact with the sensor. Further enhancement of the spatial resolution is straightforward, using more filaments at smaller distances and/or also by using thinner filaments.

The research presented here offers a versatile formulation platform for manufacturing textile yarns coated with an electrically conductive surface layer. It may serve as a foundation for further research and development activities enabling industrial-scale coating at even speeds up to 800 m min^{-1} desired for mass production. The cost of the material, mainly due to the silver particles, is slightly higher than for yarn types that use silver-coated or silver nano-wires. However, the far lower consumption of solvent and the corresponding reduction in drying efforts outweighs this downside, and beyond that silver may be replaced by less valuable materials such as silver-coated glass or copper particles, without substantial loss of conductivity.[20] Additionally, the yarn's appearance may be customized to match customers' preferences, simply by incorporating small amounts of pigment to color the yarn. Here, we have used a Nylon filament as a model system but a transfer of the concept to other yarn materials, such as cotton or silk, may also be explored in future research. Moreover, the thermoplastic properties of the conductive coating layer

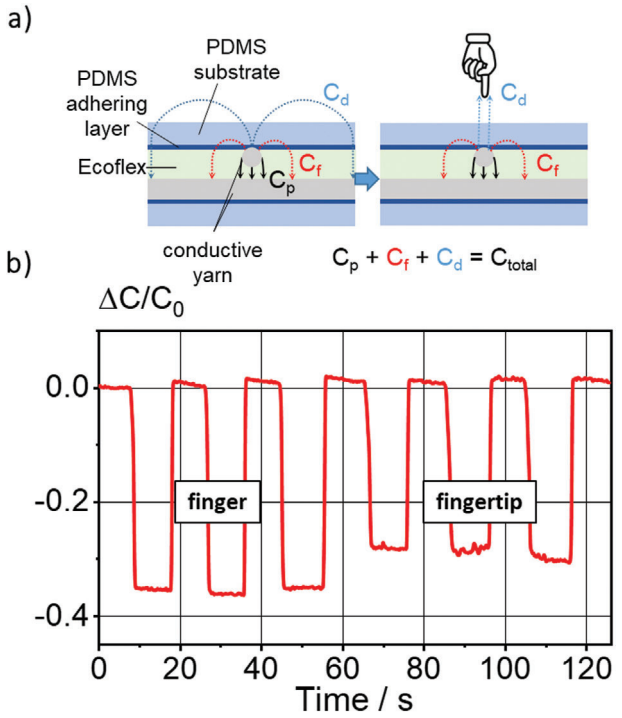

Figure 9. a) Working principle of capacitance changes caused by an approaching finger (large area) or fingertip (small area). C_{total}, C_p, C_f, and C_d represent the total sensor capacitance, plate electrode capacitance, edge capacitance in the Ecoflex overlay, and edge capacitance of the medium directly above the sensor (finger or fingertip). b) Capacitance changes over time due to an approaching finger or fingertip without applying pressure to the sensor.

may be leveraged to interconnect different sensor components without the need for solder or additional electrically conductive adhesives. Investigating this additional benefit was beyond the scope of this work. In summary, the work outlined here may set the starting point for the development of a versatile process and material platform enabling mass production of low-cost conductive yarns enabling widespread wiring and sensing applications in smart textiles.

4. Experimental Section

Formulation of the Silver-filled Polymer Solution: First, a polymer base solution, consisting of 15 wt% of the polyamide copolymer Platamid M1276 F (Arkema Specialty Polyamides, Colombes Cedex, France) dissolved in ethanol (Carl Roth, Karlsruhe, Germany), was prepared. The Platamid granules were filled together with the ethanol in a flask and stirred in a water bath at 64 °C until the granules were completely dissolved. Then, the temperature was lowered to 35 °C to store the polymer solution until the silver-filled formulation was prepared. This temperature level was chosen to avoid precipitation and to minimize the evaporation of ethanol in the process, which could alter the polymer concentration of the base solution and thus affect its coating properties. When polymer solutions with lower polymer concentrations (13 and 12 wt%) were utilized, the amount of ethanol that was added to the base solution was adjusted accordingly. Next, the plate-shaped silver particles (Ag Flake Powder Fa-S-12, DOWA Electronic Materials CO., LTD., Tokyo, Japan) with an average particle size of ≈2.5 µm were added. The size distribution and scanning electron microscopy (SEM) images of the Ag particles are displayed in Figure S4 (Supplementary Information). The amount of Ag added corresponds to 12, 15, and 20 vol% of the total nonvolatile components of the coating inks. A typical sample size was ≈10 g. In order to facilitate a uniform particle distribution, the Ag particles were suspended in the polymer solution using a noncontact planetary mixer (SpeedMixer DAC 150.1FVZ, Hauschild GmbH, Hamm, Germany). The mixing process involved a three-step mixing and cooling cycle, each lasting 2 min at 2000 rpm. Subsequently, the ionic liquid (IL) 1-Butyl-3-Methyl-imidazoliumiodide (Carl Roth, Karlsruhe, Germany) was added in varying quantities as a conductivity-enhancing agent. To facilitate precise dosing, a 25 wt% solution of the IL was prepared using the organic solvent dimethyl sulphoxide (DMSO) ≥ 99.5% (Carl Roth, Karlsruhe, Germany). Finally, the IL-DMSO mixture was added to the suspension of Ag particles in the polymer solution and mixed for an additional 1.5 min at 1700 rpm.

Yarn-Coating Process: For the coating of the Nylon yarn, the laboratory scale coating device described in Figure 1 is used. The temperature of the oven is set to 280 °C and the coating speed to 2.8 m/min. In total, a maximum of five coating layers were applied to the Nylon yarn. A table with the selection of the guiding and coating nozzle diameters is shown in Table S1 (Supplementary Information). For the coating process, ≈10 g of the silver-filled polymer solution was prepared and continuously injected with a syringe into the reservoir of the coating device.

Rheological Characterization of the Polymer Solution: The viscosity of the polymer solutions was determined at 35 °C. The measurements were conducted using a stress-controlled rotational rheometer (Physica, MCR 501, Anton Paar GmBH, Germany) equipped with a concentric cylinder geometry (inner diameter $d = 27$ mm, gap width $w = 1.13$ mm) and the viscosity η was determined in the shear rate range $1\ s^{-1} < \dot{\gamma} < 00\ s^{-1}$.

Electrical Conductivity Measurement: In order to determine the electrical conductivity of the dry Ag-filled polymer composite, the coating inks were applied to glass slides in thin layers, followed by a solvent evaporation step on a heating plate at 100 °C for 5 min in order to remove all the volatile components. Samples consisting of two layers meeting a total coating thickness of ≈70 µm were prepared, and the films were cut into strips with a length of 4 cm and a width of 0.5 cm in order to determine electrical conductivity. The actual geometry (length l, thickness t, width w) of each sample was determined precisely using an outside micrometer. The electrical resistance was determined using a four-point probe (RLC 200, Grundig, Germany). From the electrical and geometrical data, the electrical conductivity was calculated as:

$$\kappa = \frac{d_{probes}}{R \times w_{coating} \times t_{coating}} \quad (1)$$

With d_{probes} the distance of the voltage probes, $w_{coating}$ the width and $t_{coating}$ the thickness of the coating, and R the absolute electrical resistance.

Resistance Measurement of the Yarn: To measure the resistance of the coated yarn, the electrical resistance per unit length was determined. For this purpose, a 6 cm long piece of yarn was clamped between two electrodes using a customized 3D-printed yarn holder. These electrodes were connected to a Fluke 287 True-RMS Electronics Logging Multimeter (Fluke, Everett, USA), in order to measure the resistance of the yarn section (see Figure S5, Supporting Information).

Bending Test: The bending tests were conducted using a tensile testing machine (TA.XT.plus Texture Analyser, Winopal GmbH, Elze, Germany). The experimental setup is illustrated in Figure S6 (Supplementary Information). Six yarn samples were clamped in parallel into a holder and attached to the upper holder of the device. The yarn was then deflected from a vertical to a horizontal direction over a roller with a diameter of 45 mm and clamped into another holder, which could be moved back and forth along two rails and was loaded with a 225 g weight at the rear. Due to the weight, the yarn was always kept in a tensioned state. The yarn samples were then cyclically moved up and down at a speed of 17 mm s^{-1} at the upper holder, with the yarn being moved along by the movable rail and bent over the roller. Resistance measurements, as described in the section *Resistance Measurement of the Yarn* were conducted and evaluated before the test and after 300, 1200, and 3600 repeating bending cycles.

Washing Test: For the washing test, six ≈12 cm long coated yarn pieces were placed in a cotton bag and washed in a household washing machine (Express Edition Serie 4, Robert Bosch Hausgeräte GmbH, Munich, Germany) at 40 °C for 50 min and spun at 1200 revolutions per minute. Afterward, the yarn was air-dried. Before the first washing cycle and after each subsequent trial, the resistance of the yarn pieces was measured and evaluated as described in the section *Resistance Measurement of the Yarn*.

Light Microscopy Observation: To investigate the surface quality of the coated yarn, an optical microscope (Keyence VHX-6000, Keyence Corporation, Japan) was utilized.

SEM Observation: The Ag particles and the morphology of the coating layers on the yarn were imaged using scanning electron microscopy (SEM) (S-4500; Hitachi High-Technologies Europe GmbH, Krefeld, Germany).

Sensor Manufacturing: The pressure sensor was fabricated using two yarns (length: 60 mm) as the electrodes and PDMS films (Sylgard 184, Dow Corning Corp., Midland, USA) (thickness: 300 µm; size: 20 mm × 20 mm) as substrates. A PDMS resin (thickness: 10 µm) was applied to the PDMS substrate as an adhesive layer and fixed the yarns on the substrate. The first patterned substrate was coated with 120 µm thick Ecoflex (00-10, Smooth-On Inc., Macungie, U.S.A.), and the second substrate was subsequently pressed orthogonally on top of it. After that, it was cured at 80 °C for 30 mins, and the capacitive sensor was formed, as shown in Figure 6a). In addition, a yarn sensor array was prepared using ten filaments (length: 100 mm) as the electrodes and PDMS films (thickness: 300 µm; size: 55 mm × 55 mm) as substrates. The preparation process was similar to before, and a 5 × 5 array was formed, as shown in Figure 8.

Sensor Performance Tests: A customized test platform was used to analyze the performances of the sensors, based on a pressure sensor (ULC-2 N, Interface Inc., Scottsdale, America) and a z-axis displacement lifting platform. An LCR Meter (E4980AL, Keysight Technologies, Santa Rosa, America) was used to measure the electrical properties of the sensors, particularly the load-dependent change in capacitance $\Delta C/C_0$.

Supporting Information

Supporting Information is available from the Wiley Online Library or from the author.

Acknowledgements

Basic funding of the Institute for Mechanical Process Engineering and Mechanics at Karlsruhe Institute of Technology provided by the State of Baden-Württemberg. The National Nature Science Foundation of China (No. 51861135105), and Fund of Robot Technology Used for Special Environment Key Laboratory of Sichuan Province (22kftk02). The manuscript was written through the contributions of all authors. All authors have given approval to the final version of the manuscript.

Open access funding enabled and organized by Projekt DEAL.

Conflict of Interest

The authors declare no conflict of interest.

Data Availability Statement

The data that support the findings of this study are available from the corresponding author upon reasonable request.

Keywords

conductive coating, flexible fabric, high conductivity, high process speed

Received: September 18, 2024
Revised: November 11, 2024
Published online:

[1] L. Gan, Z. Zeng, H. Lu, D. Li, K. Wei, G. Cai, Y. Zhang, *SmartMat* **2023**, *4*, 1151.
[2] J. Xiong, J. Chen, P. S. Lee, *Adv. Mater.* **2021**, *33*, 2002640.
[3] S. Uzun, M. Han, C. J. Strobel, K. Hantanasirisakul, A. Goad, G. Dion, Y. Gogotsi, *Carbon* **2021**, *174*, 382.
[4] X. Shi, Y. Zuo, P. Zhai, J. Shen, Y. Yang, Z. Gao, M. Liao, J. Wu, J. Wang, X. Xu, Q. Tong, B. Zhang, B. Wang, X. Sun, L. Zhang, Q. Pei, D. Jin, P. Chen, H. Peng, *Nature* **2021**, *591*, 240.
[5] H. Sun, Z. Han, N. Willenbacher, *ACS Appl. Mater. Interfaces* **2019**, *11*, 38092.
[6] Y. Jang, S. M. Kim, G. M. Spinks, S. J. Kim, *Adv. Mater.* **2020**, *32*, 1902670.
[7] T. Lim, H. J. Kim, H. Zhang, S. Lee, *Smart Mater. Struct.* **2021**, *30*, 075006.
[8] H. Sun, J. Zettl, N. Willenbacher, *Addit. Manuf.* **2023**, *78*, 103872.
[9] T. Agcayazi, K. Chatterjee, A. Bozkurt, T. K. Ghosh, *Adv Materials Technologies* **2018**, *3*, 1700277.
[10] A. Lund, Y. Wu, B. Fenech-Salerno, F. Torrisi, T. B. Carmichael, C. Müller, *MRS Bull.* **2021**, *46*, 491.
[11] D. Cottet, J. Grzyb, T. Kirstein, G. Troster, *IEEE Trans. Adv. Packag.* **2003**, *26*, 182.
[12] S. Shang, X. Yang, X. Tao, S. S. Lam, *Polym. Int.* **2010**, *59*, 204.
[13] X. Pu, L. Li, H. Song, C. Du, Z. Zhao, C. Jiang, G. Cao, W. Hu, Z. L. Wang, *Adv. Mater.* **2015**, *27*, 2472.
[14] Y.-H. Chen, C.-C. Hsu, J.-L. He, *Surf. Coat. Technol.* **2013**, *232*, 868.
[15] Y. Tang, B. Guo, M. A. Cruz, H. Chen, Q. Zhou, Z. Lin, F. Xu, F. Xu, X. Chen, D. Cai, B. J. Wiley, J. Kang, *Adv. Sci. (Weinh)* **2022**, *9*, 2201111.
[16] S. Zhu, M. Wang, Z. Qiang, J. Song, Y. Wang, Y. Fan, Z. You, Y. Liao, M. Zhu, C. Ye, *Chem. Eng. J.* **2021**, *406*, 127140.
[17] B. Hwang, A. Lund, Y. Tian, S. Darabi, C. Müller, *ACS Appl. Mater. Interfaces* **2020**, *12*, 27537.
[18] J. Hagedorn, F. S.-L. Blanc, J. Fleischer, *Handbuch der Wickeltechnik für hocheffiziente Spulen und Motoren: Ein Beitrag zur Energieeffizienz*, 1st edn., Springer-Verlag, Berlin, Heidelberg, **2016**, pp. 129–134.
[19] C. Li, Q. Li, X. Long, T. Li, J. Zhao, K. Zhang, E. Songfeng, J. Zhang, Z. Li, Y. Yao, *ACS Appl. Mater. Interfaces* **2017**, *9*, 29047.
[20] J. Marten, M. Schnaiter, Y. Zemen, L. Podlowski, S. Ricken, N. Willenbacher, *Sol. Energy Mater. Sol. Cells* **2024**, *273*, 112966.
[21] G. Habenicht, *Kleben*, 6th edn., Springer, Berlin, Heidelberg, **2009**, p. 225.
[22] S. Chen, S. Liu, P. Wang, H. Liu, L. Liu, *J. Mater. Sci.* **2018**, *53*, 2995.
[23] Axalta, can be found under, https://www.axalta.com/electricalinsulation_global/en_US/wire-enamels/what-are-wire-enamels.html (accessed: March 2024).
[24] Y. Atwa, N. Maheshwari, I. A. Goldthorpe, *J. Mater. Chem. C* **2015**, *3*, 3908.
[25] Y. Zang, F. Zhang, C. Di, D. Zhu, *Mater. Horiz.* **2015**, *2*, 140.
[26] H. Zhang, X. Chen, Y. Liu, C. Yang, W. Liu, M. Qi, D. Zhang, *ACS Appl. Mater. Interfaces* **2024**, *16*, 2554.
[27] C. Dong, Y. Bai, J. Zou, J. Cheng, Y. An, Z. Zhang, Z. Li, S. Lin, S. Zhao, N. Li, *Nondestructive Testing and Evaluation* **2024**, 1.